Vein genesis and the emergent geomechanical behaviour of numerically simulated intact veined rock specimens under uniaxial compression

Émélie Gagnon & Jennifer J. Day
Department of Geological Sciences and Geological Engineering – Queen's

GeoCalgary 2022 October 2-5 Reflection on Resources

ABSTRACT
Many underground mining excavations are built in massive hydrothermal rockmasses where healed discontinuities (veins) can control failure. Depending on the growth mechanisms and environmental conditions at formation, macroscopically identical veins can exhibit a spectrum of different internal textures. In this study, the genesis of different vein types is used to identify nine primary micromorphologies and investigate their influence on the macromechanical behaviour of veins. Uniaxial compressive stress (UCS) tests of intact veined rock specimens containing a single calcite vein with explicit grain structure were simulated using 2D grain-based finite element method (FEM) numerical models. The results demonstrate that veins with two growth planes, high aspect-ratio grains, and anisotropic grain arrangements effect weaker macroscopic strength. Crystal-bridged veins with large grains exhibit the strongest peak strength.

RÉSUMÉ
De nombreuses excavations minières souterraines sont construites dans des masses rocheuses hydrothermales massives où les fissures minéralisées (veines) peuvent contrôler la rupture. Selon les mécanismes de croissance et les conditions environnementales lors de leur formation, des veines identiques à l'échelle d'un spécimen peuvent être formées de plusieurs textures différentes. Dans cette étude, la genèse de différents types de veines est utilisée afin d'identifier neuf micromorphologies primaires et d'étudier leur influence sur le comportement macromécanique des veines. Des essais de compression uniaxiale (UCS) d'échantillons de roche veinée intacte contenant une seule veine de calcite avec une structure de grain explicite ont été simulés à l'aide de modèles numériques microstructurels d'éléments finis (FEM) en 2D. Les résultats démontrent que les veines ayant deux surfaces de croissance, des grains à haut rapport d'aspect, et des arrangements de grains anisotropes ont une force macroscopique réduite. Les veines avec de gros grains trapus sont les plus fortes.

1 INTRODUCTION

The presence of veins is pertinent in massive to moderately jointed rockmasses as underground engineering projects go deeper, and the complexity of ground stresses tends to increase. In these environments, a challenge during site investigation is identifying healed discontinuities that have opened during drilling activities, which can lead to a mischaracterization of rockmass structure and result in overly conservative ground support design or in the case of block cave mining, the calculation of optimistic but inaccurate fragmentation potentials (Kaiser et al. 2015). From a safety perspective, veins can be a driving factor in violent failure phenomena such as rockbursts due to elasticity contrasts between the discontinuity and host rock (Robbiano, 2022; Han et al. 2021).

Mineral veins and veinlets are defined in this context as healed discontinuities ranging from less than 1 cm to 10 cm in width that form by mineral precipitation from hydrothermal fluids, and are usually thought of as mesoscopic heterogeneities that occur within blocks of intact rock bounded by fractures, termed intrablock structures by Day et al. (2019). From an elemental perspective, it is widely accepted that brittle rock fracture mechanics are controlled by the presence of heterogeneities at the grain scale (Diederichs 2003; Potyondy and Cundall 2004; Lan et al. 2010). Mineral veins have a variety of morphologies depending on the geological conditions that led to their formation. They are often studied by structural and economic geologists to gain information about the hydrological and kinematic histories of a rockmass.

Improving the understanding of the geometric heterogeneity of veins at a grain scale, from a geomechanics perspective, and how this impacts fracture mechanics is beneficial to better anticipate the in situ strength and failure behaviour of veined rockmasses. In this study, uniaxial compressive stress (UCS) tests of intact veined rock specimens are simulated using two-dimensional (2D) continuum grain-based finite element method (FEM) numerical models to investigate the emergent behaviour of veins that are identical at a macroscopic level (i.e. specimen scale) but have different microfabrics.

1.1 Characterization and Mechanics of Veined Rocks

The topic of veined rock mechanics is a relatively new field of research that was initiated by the expansion of Chilean porphyry cave mines at great depths in the 2000s and 2010s (e.g. Brzovic and Villaescusa 2007; Day 2019; Day et al. 2014, 2015, 2019; Turichshev and Hadjigeorgiou 2015, 2017). Before this, little attention had been given to veins as most excavations were built in jointed rockmasses where open discontinuities control failure. As brittle rockmasses become massive with increasing depth, skarn, stockwork, hydrothermal, and tectonic veins can control failure due to the elasticity and strength contrasts with the host rock. The main challenges in characterizing veined rockmasses are the high density and apparent stochasticity

of veins at the excavation scale and the number of integrative factors that must be considered (e.g. infill and wall-rock composition, vein thickness, persistence, spacing, orientation, network density, and orientation of the stress field).

Laboratory testing is useful to characterize the stress-strain response of an intact veined rock specimen but is restricted by cost and labour, lacks replicability, and the results depend on the unique heterogeneity in the chosen specimen. Therefore, it has been impossible to empirically establish a tangible understanding and constitutive framework of the in situ strength and failure modes of veined rockmasses that can be applied to different scenarios. Characterization tools have been modified to consider healed intrablock structures, but these methods are subjective and still require extensive site-specific modifications relying on engineering judgment (Day et al. 2019; Bewick et al. 2019).

Heterogeneity at the mineral grain scale leads to localized stress gradients and plays a key role on fracture mechanics (Diederichs 2003). If we were able to resolve the composition of rockmasses at the grain scale and perform first principle calculations based on established laws of physics, all emergent failure modes should theoretically be anticipated.

In recent years, increased computational power has made it possible to perform grain-based modelling of rocks. Lan et al. (2010) presented microstructural heterogeneity in three categories: (i) microgeometric heterogeneity (grain size and shape), (ii) microelastic heterogeneity (Young's modulus, E, and Poisson's ratio, v, contrasts between the constituent grains), and (iii) microcontact heterogeneity (length and orientation of contacts, stiffness). They found that microgeometric heterogeneity affects the Crack Initiation (CI) brittle damage threshold of a rock. Further research on microgeometric heterogeneity has found that the aspect ratio of crystals plays a significant role in the density of microcracks formed within them during loading (Ghasemi et al. 2020). While some veined rocks have been simulated using grain-based models, to the knowledge of the authors, the geometric heterogeneity of veins at a grain scale, which is the focus of this research, has not yet been studied in the field of rock mechanics.

1.2 Vein Microstructure

Mineral veins exhibit a variety of microstructure depending on their formation mechanisms. While most research in geomechanics has focused on veined rocks at laboratory or greater scales, vein micromorphologies have been studied extensively in structural geology as they provide information about the mechanical and hydraulic history of a rockmass (Bons et al. 2012; Spruzeniece et al. 2021). Several parametric studies have evaluated the influence of boundary conditions on crystal growth in mineral veins (Hilgers et al. 2001; Bons 2001; Spruzeniece et al. 2021). Fracture formation (rate, aperture, roughness of surface), fluid transportation mechanisms (advection or diffusion), and hydraulic conditions (temperature, velocity, pressure, saturation) are all factors that control precipitation of vein infill (Ankit et al. 2013).

Veins are classified into one of two main groups, antitaxial or syntaxial, depending on the location of grain nucleation. Antitaxial veins grow from a characteristic median zone towards the wall rock. These veins are thought to form in narrow fractures that suppress growth competition and the development of crystal facets. The grains grow in minute increments, obtaining large length to width ratios such that these veins are often described as fibrous. Syntaxial veins are initially formed by the nucleation of mineral grains on the wall rock, with subsequent growth towards the centre of the vein. An example of a syntaxial vein in petrographic thin section is presented in Figure 1. As veins are formed in tectonic environments, fractures can repeatedly localize along the same discontinuity surface if the rate of strength increase from healing is slower than the rate of crack propagation. The cyclic process of mineral precipitation in a vein and reopening of the discontinuity is referred to as the crack-seal process. The number and location of crack-seal events play a key role in the resulting microstructure of syntaxial veins (Bons et al. 2012). It is impossible to appropriately cover the multifarious subject of vein microstructure in a few paragraphs. While brief descriptions of the factors that cause certain vein morphologies are provided below, interested readers are referred to the works of Passchier and Trouw (2005) and Bons et al. (2012) among numerous others, for in-depth discussions on the matter.

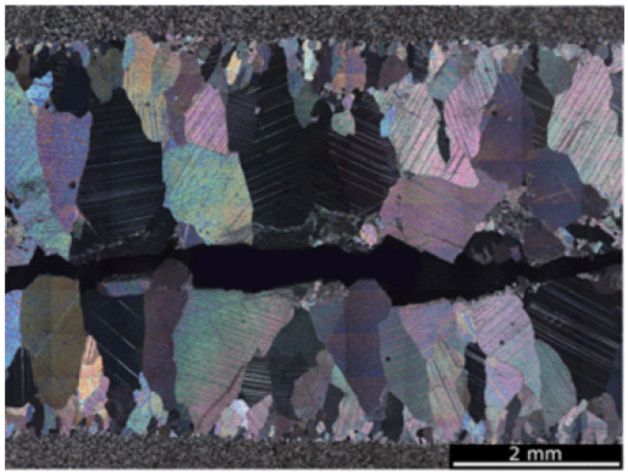

Figure 1. A syntaxial calcite vein formed by a single crack-seal event. In the context of this study, the microstructure is inward elongate blocky (Vein Type 9) (modified from Spruzeniece et al. 2021)

To observe the range of geometric microheterogeneity that exists in healed discontinuities, a database of thin sections of mineral veins was compiled from literature for this study. To characterize the vast spectrum of possible crystal arrangements, nine primary vein types were idealized and sketched to perform a practical investigation of the influence of geometric heterogeneity at a micro-scale on the macroscopic peak strength response of veins. These archetypes were selected to bound the emergent mechanical behaviour of veins that are identical at a

macro-scale but have different grain fabrics. As veins with similar fabrics can form under different environmental conditions and mechanisms, the selected patterns were classified as syntaxial or antitaxial but mostly assigned descriptive names based on the size and shape of grains, and the location of growth planes, instead of based on their genesis. The nine vein morphology types are shown in Figure 2.

The first three microstructure types are found within antitaxial veins, where growth planes are located at the centre of the veins. In Vein Type 1, the grains grew outwards at differential growth rates based on their crystallographic orientation. This resulted in the gradual widening of the faster growing grains which we have termed as an outward elongate blocky grain structure. Vein Types 2 and 3 are classical representations of the fibrous fabrics usually observed in antitaxial veins, with minimal widening of the grains away from the median zone, which is interpreted to mean there is almost no growth competition. Fibrous refers to crystals with a large length/width ratio and smooth boundaries, which in minerals that do not normally have a fibrous habit can only form if growth competition is inhibited, such as would be in the absence of an open cavity (Bons et al. 2012). Grains can lock onto asperities of the wall rock surface and deform with it. An example of this is shown in Vein Type 2 (Figure 2) where the discontinuity underwent dextral Mode II Shear deformation.

Vein Types 4, 5, and 6 are referred to as blocky in structural geology but the terms single-, double- and multi-crystal bridged are used here to avoid confusion with the rock mechanics connotation of the descriptor. Generally, the growth of existing crystals is energetically favourable to the nucleation of additional crystals. Therefore, these morphologies are thought to form due to extreme growth competition in an open cavity with fast opening rates. In the poly-crystal bridged vein (Type 6), the constituent polygonal grains are equigranular. Growth planes are not located for this vein type because grains nucleated throughout the vein.

Vein Type 7 is a stretching vein and forms during multiple crack-seal cycles where the location of the fracture plane varies throughout the vein. This results in grains with serrated grain boundaries, as the grains are cut and resealed with the same material multiple times along numerous growth planes.

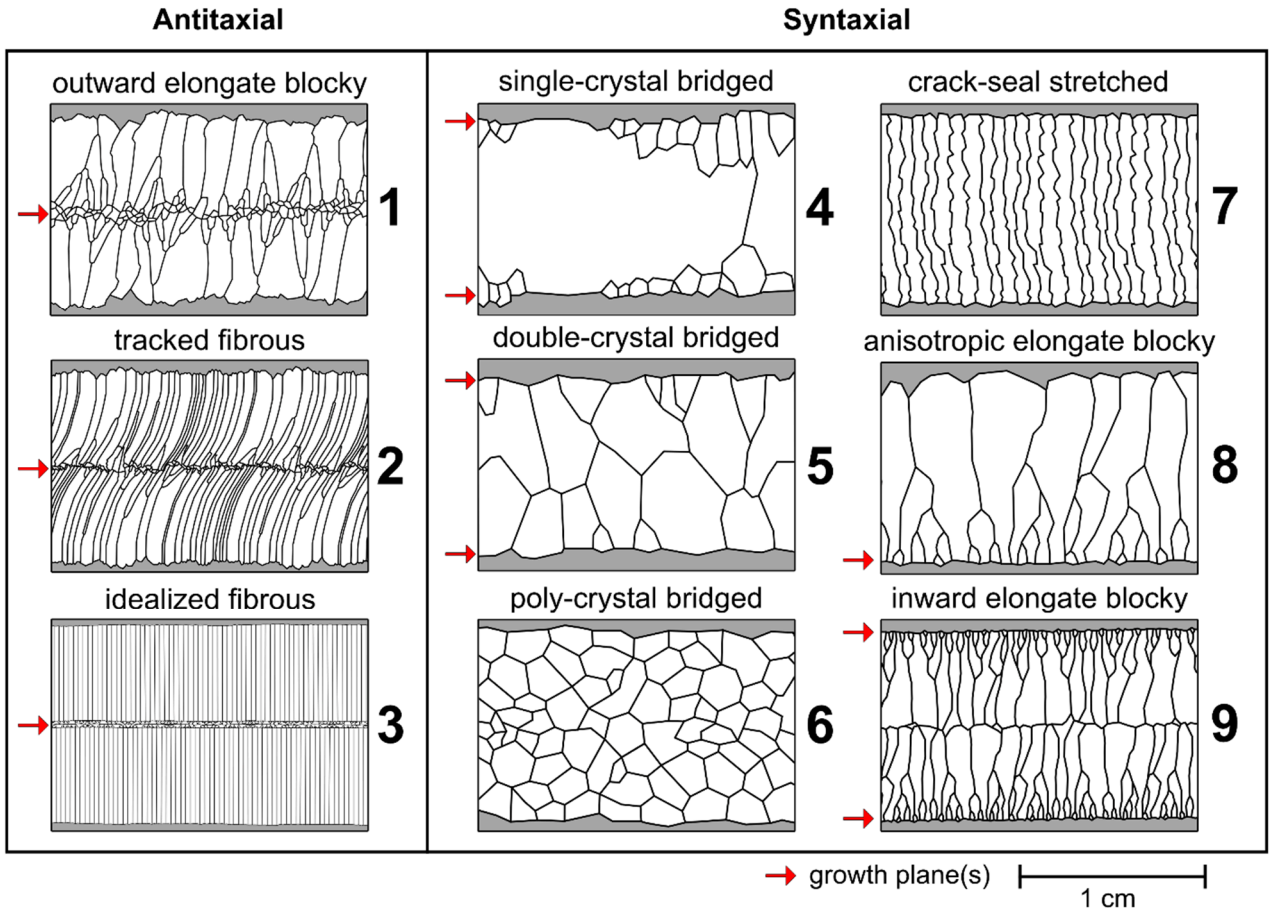

Figure 2. Vein morphologies sorted into 9 types, where Types 1-3 are antitaxial and Types 4-9 are syntaxial; antitaxial veins have a single growth plane resulting in the distinct median zone; syntaxial veins have one or more growth plane locations depending on the number of crack-seal events.

In Vein Type 8, growth was unidirectional, and a single growth plane exists which is occasionally observed in nature (Figure 2). Vein Type 9 has a similar morphology to Vein Type 1, but grains nucleated along the wall-rock contacts and grew inwards.

1.3 Continuum Grain-Based Modelling of Rocks

While grain-based modelling is traditionally done using discrete and finite-discrete element method numerical codes (DEM, FDEM), Voronoi-grain models using the finite element method (FEM) are more accessible alternatives that can be beneficial at the conceptual stages of a study. The computational efficiency of continuum codes accelerates the calibration process while still capturing the important characteristics of brittle rock failure (Li and Bahrani 2021; Rogenes et al. 2021; Markus and Diederichs 2022). The FEM models used in this study are described in the following section.

2 MODEL CONFIGURATION

To isolate the influence of vein microstructure on the emergent fracture patterns of veined rocks, continuum grain-based models of UCS specimens containing a centrally located vein dipping at 45° were prepared while respecting the ISRM suggested method (Fairhurst and Hudson 1999). A vein thickness of 1 cm was selected to provide ample resolution of the microfabric and minimize grain size contrasts between the host and vein rock that could lead to differential stress concentrations. Specimen geometries including vein microstructure were imported directly into RS2 by Rocscience (2021) and are presented in Figure 3.

A Voronoi joint network of medium regular polygons was used to simulate grains with an average diameter of 1.6 mm in the host rock. The joint network was generated using an identical randomized seed value for all specimens, ensuring the geometric microheterogeneity of the vein was the only varying factor between samples. Quasi-static uniaxial compressive loading was simulated

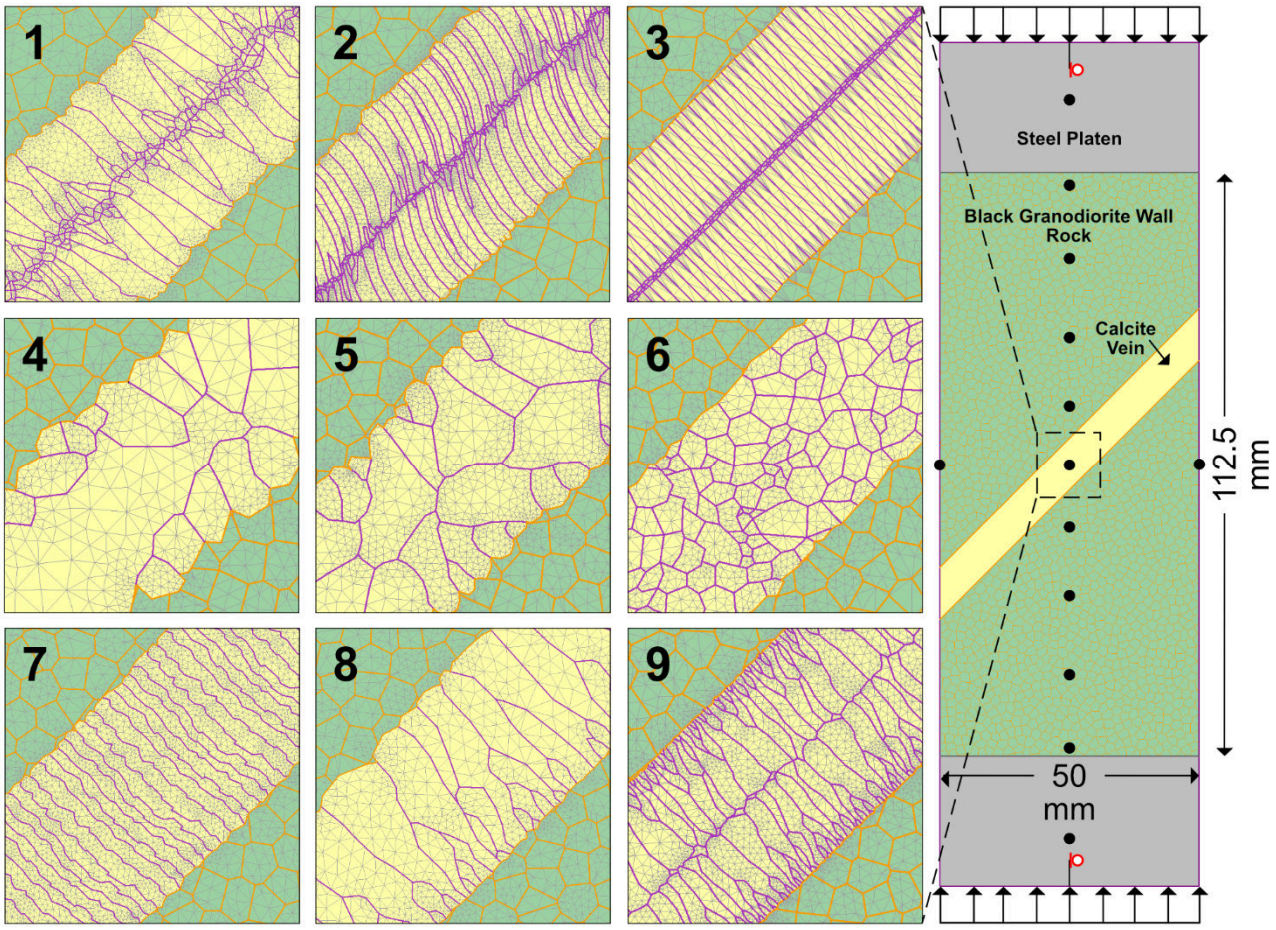

Figure 3. The overall model set-up showing steel platen (grey), wall rock (green material with orange Voronoi network grain boundaries), and vein geometries (yellow), as well as boundary conditions; detailed views of all 9 meshed Vein Types with discrete microstructure boundaries defined by joint elements (purple) and grain material (yellow) with triangular mesh; Vein Types 1-3 are antitaxial, and Vein Types 4-9 are syntaxial.

by applying a constant displacement of 0.003 mm at the top and bottom of the specimen over 100 sequential stages. A graded mesh of 6-noded triangles discretized using 200 points, with a window of increased discretization density defined 5 mm around the vein was used to converge to the macroscopic peak strength while minimizing computational time.

The material properties of the specimens were matched to the Black granodiorite unit from the Legacy Skarn deposit in New Brunswick, Canada, because mining excavations are commonly built in igneous rockmasses with similar properties, this lithology is known to contain ubiquitous calcite veining, and both homogeneous and veined samples have been tested under uniaxial stress conditions in the laboratory (Clark and Day 2021). Calcite veins are common in numerous rockmasses and can exhibit all the Vein Types shown in Figure 2. The average UCS reported for homogeneous specimens of the Black granodiorite is 250 ± 30 MPa. The rock has a Young's Modulus (E) of 65 ± 3 GPa and a Poisson's Ratio (v) of 0.25 (Clark and Day 2021). A tensile strength of 10 MPa was estimated based on Perras and Diederichs (2014).

2.1 Calibration of the Model Micro-Parameters

Predictive numerical modelling in rock mechanics is usually done after characterization of the input material properties through site investigation and laboratory testing. A major component of published grain-based models is the calibration of grain and grain boundary properties such that the emergent macroscopic behaviour replicates the elastoplastic response of physical samples that were tested under the same stress conditions (Li and Bahrani 2021; Rogenes et al. 2021). No physical specimens of the Legacy Skarn's Black granodiorite exist with the particular vein configurations simulated in this study; therefore, the calibration process focused on selecting micro-parameters that effect behaviours typical of brittle rocks and provide the opportunity for meaningful observations.

Black granodiorite is composed of Quartz (50%), Albite (37%), Clinochlore (8%), and Muscovite (2%) (Clark and Day 2021). The granodiorite was modelled here using homogeneous grains defined by Voronoi joint network boundaries to simplify model set-up and moderate the number of unknowns. This simplification is trivial in the context of this study (Sinha and Walton 2020).

The initial elastic parameter (E,v) and density (ρ) values used for the granodiorite were obtained by calculating a weighted average of published properties of the four constituent minerals (Alexandrov and Ryshova 1961; Bass 1995). The Mohr-Coulomb constitutive model was used to define the strength of the grain material and grain boundaries. As a starting point, tensile strength (σ_T), friction angle (φ), and cohesion (c) values were obtained for the granodiorite by fitting a Mohr-Coulomb envelope to the target material properties obtained during laboratory testing.

The normal stiffness of the granodiorite grain boundaries was set to $E \cdot 10^3$ GPa/m. As this is an underdetermined problem, the micro-parameters selected are a non-unique solution that represent the macroscopic behaviour. The following simplification and postulation attempts were made to reduce the number of unknowns and select values for the remaining parameters using logical reasoning as opposed to simple trial and error:

- Most cracks are intergranular at low confinements; therefore, the properties of the grain boundaries are set to be weaker than those of the grains themselves, and intragranular heterogeneities such as cleavage planes are omitted (Ghasemi et al. 2020).
- The calcite infill is slightly weaker and softer than the host wall rock which should be reflected in the grain and grain boundary parameters.
- The vein-wall rock (VW) contacts between calcite and granodiorite grains are set to be identical to those within the granodiorite.
- The platens are modelled elastically as the applied load should be inconsequential relative to the strength of the case-hardened alloy steel.
- The ratio of normal stiffness (K_n) to shear stiffness (K_s) for the grain boundaries is assumed to be 1.5. Load is almost entirely normally distributed along the platen-specimen contact, thus $K_n/K_s = 10$ for this contact.
- The grain boundaries follow a cohesion-weakening friction-strengthening (CWFS) strength model (Hajiabdolmajid et al. 2002). Friction is initially set to 20° and mobilizes to the ϕ value determined using the Mohr-Coulomb constitutive model after cohesive bonds break. The initial CWFS parameters were obtained using the procedure described by Walton (2019).
- For the grains themselves, residual tension and cohesion are set to 0, and the friction angle remains constant. This is a commonly accepted simplification as the tensile and cohesive forces that do remain after fracturing are infinitesimal (Markus & Diederichs 2022).

Firstly, a homogeneous specimen (without a vein) was simulated and calibrated to the macroscopic peak strength and elastic properties of the Black granodiorite. Microproperties were varied until the emergent peak strength and elastic moduli of the specimen were within 10% of the average physical values reported by Clark and Day (2021).

Secondly, a veined specimen with a Voronoi joint network discreetly representing the vein fabric was used to ensure that the properties chosen for the calcite grains within the vein yielded reasonable results. The average UCS of the veined Black granodiorite specimens tested in the laboratory is 170 MPa, with values ranging from 120 MPa to 210 MPa (Clark and Day 2021). The emergent strength of the modelled veined specimen was 150 MPa. The veins were thinner than 1 mm in the physical specimens, thus the lower peak strength value observed in the model is deemed reasonable for a specimen containing a 1 cm thick vein. The calibrated microproperties used in this study are listed in Table 1.

Table 1. Microproperties used in the veined UCS model

Grain Properties	ρ (g/cm^3)	E (GPa)	v	σ_t (MPa)	c (MPa)	Φ (°)
Vein: Calcite	2.71	63	0.24	13	60	45
Host rock: Granodiorite	2.64	65	0.15	17	80	55
Platens: Steel	7.85	200	0.3	500	10.5	35

Grain Boundary Properties	K_n (GPa/m)	K_s (GPa/m)	σ_t (MPa)	c (MPa)	Φ (°)
Platen-Specimen	20000	2000	0	0	35
Granodiorite & VW	65000	43333	15 (0)*	60 (3)*	20 (65)*
Calcite-Calcite	55000	36666	12 (0)	50 (2)*	20 (45)*

*Note: bracketed values are residual properties

6 MODEL RESULTS

The simulated UCS test results for veined specimens with varying microstructure are summarized in Table 2. Axial stress and axial strain results were calculated as an average value from query points shown in Figure 3. The axial stress-strain curves for each modelled specimen are shown in Figure 4. The yielded finite elements at the stage where failure occurred are presented in Figure 5. Yielded joint elements, yielded material elements, major principal stresses (σ_1), horizontal and vertical displacement, and volumetric strain were used to interpret the results of each analysis.

The peak strength values that emerged vary by 37% between all specimens (99 MPa to 157 MPa).

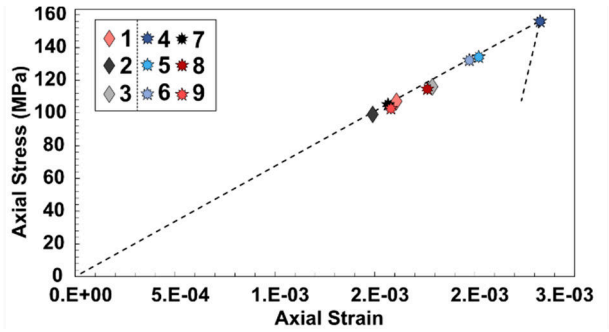

Figure 4. Axial stress-strain results for each veined specimen, where diamond and stars represent specimens with antitaxial and syntaxial veins, respectively.

The overall failure surface in each specimen is interpreted by sequentially analyzing the progressive yielding of elements within the specimen. Yielded mesh elements within the continuous material are interpreted to represent intragranular cracks and yielded joints elements represent intergranular cracks. The spatial density and temporal accumulation of yielded elements in the specimens are used to infer zones of crack coalescence.

Specimens 1, 2, and 3 containing antitaxial veins all failed along the median zones of the veins and reached low peak strengths relative to other specimens. In Specimen 1, the initial yielded elements are concentrated within the smaller grains at the centre of the vein. All elements failed in tension and yielded joint elements prevailed. As loading progresses, stresses localized sub-vertically within the vein leading to the coalescence of cracks in this direction (Figure 5). Eventually, all the elements within the median zone of the vein yielded, and the cracks are interpreted to have coalesced into a macroscopic fracture plane through the middle of the vein. In Specimen 2, yielded elements are also concentrated within the median zone of the vein. At about 40% of the peak strength loading, yielded joint and mesh elements propagate perpendicular to the vein following the shape of individual grains. This can be observed in the bottom half of the vein (Figure 5). At failure, the entire top half of the vein yielded in tension and two fractures propagated axially splitting the specimen in two. Based on the sequential increase in yielded elements, stress and volumetric strain contours, and vertical displacement contours (Figure 5), two macroscopic failure surfaces are inferred to develop at the vein centre and along the core axis. Specimen 2 reached the lowest peak strength of 99 MPa.

In Specimen 3, yielded elements are entirely restricted to the median zone of the vein until 50% of peak strength loading. At this point, localized subvertical stress bands are observed and eight regularly spaced shear bands oriented 20° from σ_1 and 70° from the vein long-axis form along the centre of the vein (Figure 5).

Specimen 4 has the highest UCS value and yielded in combination within the vein and host rock of the specimen. Initially, most yielded elements are intergranular cracks along the vein-wall rock boundary. The coalescence of cracks that led to macroscopic failure of the specimen is interpreted to have started from the top right vein-wall rock boundary, traversed the width of the vein, and emerged on the left along the bottom vein-wall boundary. Simultaneously, axial splitting occurred through the wall rock on both sides of the vein.

Table 2. Summary of veined UCS model results

Specimen #	UCS (MPa)	Failure Stage # (/100)	Failure Mode*
1	107	60	VF – I
2	99	54	VF – I & AS
3	116	71	VF – I
4	157	81	VF – C & AS
5	132	69	VF – S
6	137	74	VF – C
7	103	61	VF – VW & S
8	115	61	VF – VW
9	105	62	VF – VW

* Vein Failure (VF), I (Through infill), VW (At vein-wall contact), C (Combination of I and VW), AS (Axial Splitting), and S (Spalling)

In Specimen 5, yielded elements initiated in proximity to the vein-wall rock contact but mostly along joints oriented sub-perpendicular to the long axis of the vein. Microcracks continued to form mostly along the grain boundaries but eventually formed within the grains, propagating parallel to the direction of loading within the vein. Formed cracks were almost entirely contained within the vein until the peak strength was reached and stresses localized at the extremities of the specimen along the vein, propagating vertically to cause spalling through the host rock.

Specimen 6 failed in combination within the vein material and along the vein-wall rock contact. Elements first yielded in a seemingly random fashion along grain boundaries throughout the vein. Eventually, subvertical lines of high density yielded joint elements were formed dipping 10° to 20° from the vertical axis within the vein. Eventually, microcracks propagated and coalesced into a failure plane like the one observed in the Type 4 vein. Outward propagation of cracks axially into the host rock is observed.

In Specimen 7, shear bands oriented 20° from loading as observed in the Type 3 vein emerge. Yielded elements then propagate laterally throughout the vein until the sample shear through the vein entirely. Contour plots of σ_1, absolute horizontal displacement, and volumetric strain of Specimen 7 at failure are included in Figure 5 to provide an example of how the macroscopic failure planes were determined. Similar to specimen 5, at the peak strength stage, stresses concentrated at the edges of the specimen along the vein and spalled vertically. The failure of this specimen is interpreted to be a combination of shear banding through the vein and spalling.

In Specimen 8, elements initially yield exclusively along the sub-vertically oriented grain boundaries of small grains located near the bottom of the vein. Elements yield sequentially upwards following the grain boundaries. At about 45% of peak loading, intragranular cracks start to form where stresses are localized vertically. The macroscopic failure surface is restricted to the bottom vein-wall rock boundary.

Specimen 9 exhibited the second minimum peak strength of all the models in this study. All yielded elements in this specimen are constrained within the vein material itself. Most of the yielded elements are located along the boundaries of the smaller grains at the extents of the vein. Intragrain yielding eventually occurs as cracks propagate vertically throughout the vein. The macroscopic failure planes are located at the vein-wall rock contacts.

7 DISCUSSION

The results of the FEM simulation of UCS tests on nine veined rock specimens with idealized microstructure show that vein micromorphology impacts the development of microcracks within the rock and the geomechanical properties at the specimen scale. By simply changing the grain geometry within the vein, otherwise identical specimens reached different peak strengths, failed at different rates, and in different modes.

As expected, the initiation and propagation of microcracks within the specimens were mostly concentrated within the weaker calcite veins. Significant initiation of cracks within the host rock itself was only observed in two specimens prior to failure: Vein Types 4 and 6. In the specimen with a Type 4 vein, the greater size of grains within the vein than in the host rock is interpreted to have contributed to the axial propagation of cracks into the wall rock. Specimens with a Type 2, 5, and 7 veins failed through the wall rock but cracks only propagated outside of the vein at failure. It is interpreted that in a physical UCS test, these specimens would fail in an explosive manner.

Veins that are symmetric about their long axis, such as the antitaxial veins (Types 1, 2, 3) and the syntaxial inward elongate block vein (Type 9) are generally weaker than veins without two growth planes. There is a high density of grain boundaries along the nucleation plane, which is where the smaller, oldest grains that were outgrown are located. This results in a localized weak surface, where stresses coalesce, and cracking propagates. The failure surface in the anisotropic elongate blocky Type 8 vein, where the microstructure is essentially half of the Type 9 vein, is also located along the nucleation plane. The increase in strength between the two specimens is attributed to the vein containing one single versus two weaker planes. Conceptually, the vein-wall rock boundary is the most likely plane of failure in antitaxial veins, as poor adhesion of the vein infill to the wall rock can lead to the presence of vugs (Ankit et al. 2013; Spruzeniece et al. 2021). A similar reasoning can be adopted for the median zone of the syntaxial Type 9 vein. The results of this study demonstrate that as symmetry along the plane of the vein increases, and stresses are localized along this plane, such as in the case of a median zone in antitaxial veins, the emergent peak strength decreases.

The emergence of the crystal-bridged veins (Types 4, 5, 6) as the strongest peak strength is attributed to the diminished influence isotropic geometry plays on stress localization. The decrease in strength between Specimen 4 and 6 is correlated with grain size. The density of grain boundaries within the vein were assigned lower strength parameters than the grain material, hence a higher density of contacts results in a weaker material. Additionally, more microcracks formed within grains with a high aspect ratio (length/width), which were prevalent in antitaxial and elongate vein types. This observation is consistent with the findings of past microstructural research (Ghasemi 2020). Further work is recommended to characterize the relative strength of mineral grains versus their contacts to improve the selection of microparameters and meaningfully quantity the expected influence of grain size on strength. Contacts between grains do not have homogeneous properties and these variations depending on the growth mechanism of grains should also be investigated.

A limitation of this study is the homogeneous nature of the grains themselves. Crystallography is a major control on the growth rate of crystals, such that grains are often oriented preferentially within veins. This is most important in veins with extreme growth competition and anisotropy, such as Type 8 and 9 veins. For a mineral such as calcite,

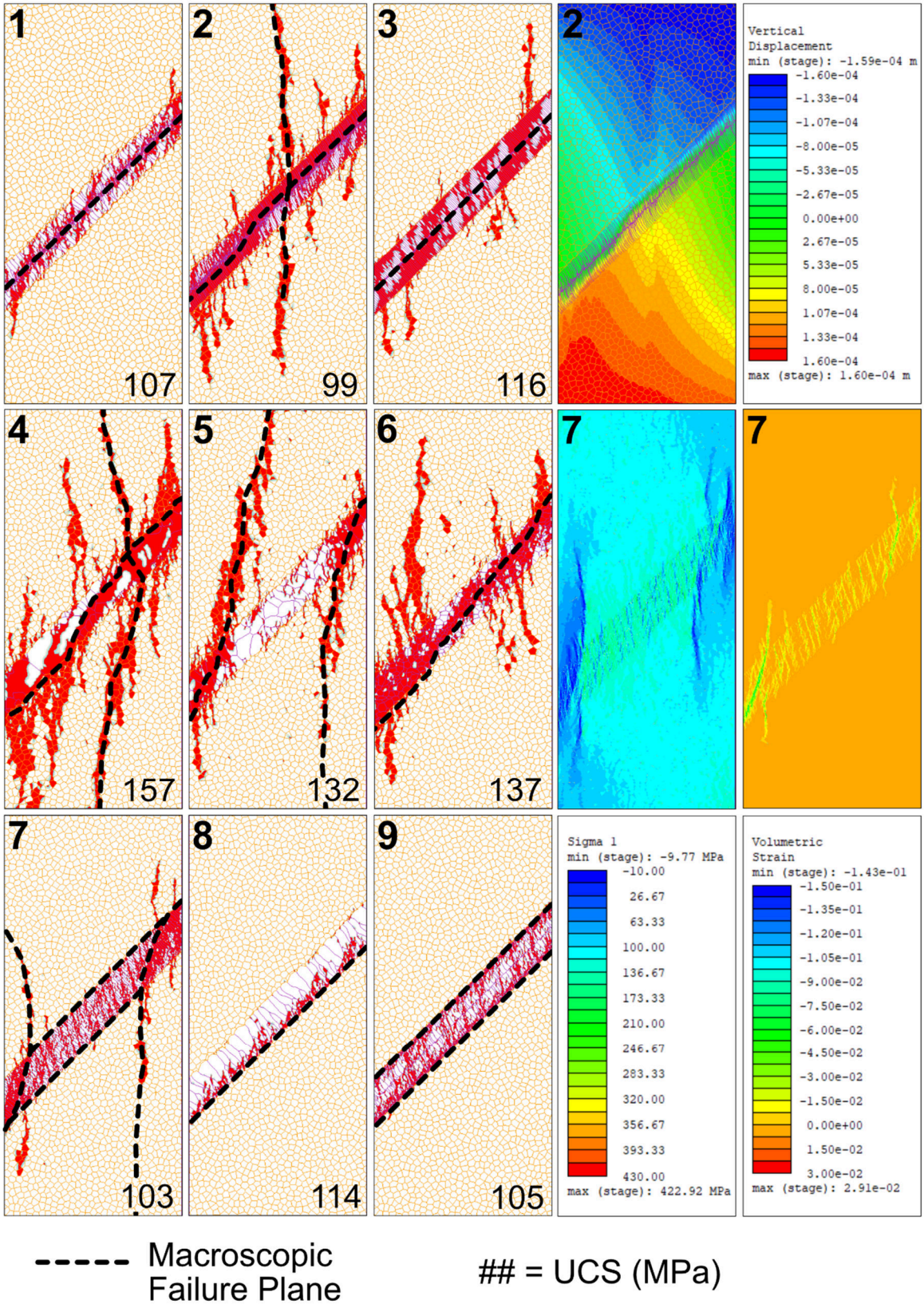

Figure 5. Model results of veined UCS specimens, showing yielded elements at failure and the interpreted failure surface(s) for all specimens, as well as example results of vertical displacement for Specimen 2, and major principal stress (σ_1) and volumetric strain for Specimen 7.

which has trigonal crystal habit, cleavage could contribute to increased intragranular cracking and change the fracture patterns of the vein. Intra-granular flaws, fluid inclusions, and selvages are all additional factors that could influence the geomechanical behaviour of veins.

Veins with different microstructures usually exhibit spatial correlation based on fracture mechanics and fluid transport mechanisms throughout a rockmass. Fibrous veins which crystallize in the absence of significant void space are hypothesized to form by diffusion mechanisms in small, segregated fractures (Oliver 2001; Bons 2012).

Fractures favourably oriented relative to the local stress field can act as important fluid conducts in which crack-seal and crystal-bridged veins are more likely to form. As the resulting morphology of veins is influenced by coupled mechanical, chemical, and kinematical factors, a single framework cannot adequately represent the distribution of vein microstructure in all networks. In most mining environments though, vein networks are already characterized by geologists during the exploration phases of a project. Categorization of vein types based on time of formation, spatial variability, geometry, and composition is often completed to understand the genesis of the deposit and quantify ore resources. By improving our understanding of the range of characteristics that influence the strength of a vein in geological terms, such as micro-morphology, rock engineering practitioners will be able to harness information available from geoscience colleagues (e.g. structural and exploration geologists) and gain greater insight into which healed discontinuities may be expected to control failure during construction.

5 CONCLUSIONS

The characterization of veined rocks is usually completed at the laboratory and rockmass scales in engineering. That being said, veins with identical geometries and composition at these scales can exhibit different microstructure based on the geological conditions that led to their formation. In this study, UCS tests on nine veined rock samples with different micro-morphologies were numerically simulated using 2D Voronoi-grain FEM models. Factors that lead to the genesis of different vein types were used to create a framework to categorize geometries of microstructural fabrics. The impact of the nine vein types in this framework on vein geomechanical behaviour were investigated. Results showed that veins with two growth planes and anisotropic grain arrangements resulting from growth competition effect weaker macroscopic strength. Vein types termed crystal-bridged in this study (referred to as blocky in structural geology) exhibited the highest strengths due to the relative sphericity and disordered arrangements of their constituent grains which are less favourable for crack initiation and propagation.

Overall, furthering our understanding of geomechanical vein behaviour at the microscale will enable more meaningful interpretation of laboratory testing results on veined rock specimens, in turn leading to improved rockmass characterization and engineering decision-making.

ACKNOWLEDGMENTS

This research was financially supported by the Natural Sciences and Engineering Research Council of Canada (Discovery Grant, PI: Day). Thank you to Mark Mcdonald for his constructive reviews of this paper.

REFERENCES

Alexandrov, K.S. and Ryshova, T.V. 1961. The Elastic Properties of Rock-Forming Minerals. *II: Layered Silicates. Bulletin USSR Academy of Science, Geophysics Series 9*, 12: 1165-1168.

Ankit, K., Nestler, B., Selzer, M., and Reichardt, M. 2013. Phase-field study of grain boundary tracking behaviour in crack-seal microstructures. *Contributions to Mineralogy and Petrology,* 166: 1709-1723. DOI 10.1007/s00410-013-0950-x

Bass, J.D. 1995. Elasticity of Minerals, Glasses, and Melts. In *Mineral Physics & Crystallography*, T.J. Ahrens (Ed.).

Bewick, R.P., Campbell, R., Brzovic, A., Schwarz A., and Pierce, M. 2019. Incorporating veined rock mass characteristics into engineering design and caving. *53rd US Rock Mechanics/Geomechanics Symposium*, ARMA, New York, NY, USA, pp.11.

Bons, P.D. 2001. Development of crystal morphology during unitaxial growth in a progressively widening vein: I. The numerical model. *Journal of Structural Geology*, 23: 865-872. DOI 10.1016/S0191-8141(00)00159-0

Bons, P.D., Elburg, M.A., and Gomez-Rivas, E. 2012. A review of the formation of tectonic veins and their microstructures. *Journal of Structural Geology*, 43: 33-62. DOI 10.1016/j.jsg.2012.07.005

Brzovic, A., and Villaescusa, E. 2007. Rock mass characterization and assessment of block-forming geological discontinuities during caving of primary copper ore at the El Teniente mine, Chile. *International Journal of Rock Mechanics & Mining Sciences*, 44: 565-583. DOI 10.1016/j.ijrmms.2006.09.010

Day, J.J. 2019. Brittle overbreak prediction in deep excavations for hydrothermally altered and heterogeneous rockmasses. *Bulletin of Engineering Geology and the Environment*, 79: 1041-1060 (2020). DOI 10.1007/s10064-019-01578-z.

Day, J.J., Diederichs, M.S. and Hutchinson, D.J. 2014. Component and system deformation properties of complex rockmasses with healed structure. *48th U.S. Rock Mechanics Geomechanics Symposium*, ARMA, Minneapolis, MN, USA, 11p.

Day, J.J., Diederichs, M.S. and Hutchinson, D.J. 2015. Common Core: Core logging procedures for characterization of complex rockmasses as input into geomechanical analysis for tunnel design. *Tunnels and Tunnelling*, 1: 26-32.

Day, J.J., Diederichs, M.S., and Hutchinson, D.J. 2017. New direct shear testing protocols and analyses for fractures and healed intrablock rockmass discontinuities. *Engineering Geology*, 229: 53-72. DOI 10.1016/j.enggeo.2017.08.027.

Day J.J., Diederichs, M.S, and Hutchinson, D.J. 2019. Composite Geological Strength Index approach with application to hydrothermal vein networks and other intrablock structures in complex rockmasses. *Geotechnical and Geological Engineering*, 37: 5285–5314. DOI 10.1007/s10706-019-00980-4.

Diederichs, M.S. 2003. Rock Fracture and Collapse Under Low Confinement Conditions. *Rock Mechanics & Rock Engineering,* 36: 339-381. DOI 10.1007/s00603-003-0015-y

Fairhurst, C.E. and Hudson, J.A. 1999. Draft ISRM suggested method for the complete stress-strain curve for intact rock in uniaxial compression. *International Journal of Rock Mechanics and Mining Sciences*, 36: 279-289.

Ghasemi, S., Khamehchiyan, M., Taheri, A., Nikudel, M.R, and Zalooli, A. 2020. Crack Evolution in Damage Stress Thresholds in Different Minerals of Granite Rock. *Rock Mechanics and Rock Engineering*, 53: 1163-1178. DOI 10.1007/s00603-019-01964-9

Hajiabdolmajid, V., Kaiser, P.K., and Martin, C.D. 2002. Modelling brittle failure of rock. *International Journal of Rock Mechanics & Mining Sciences,* 39: 731-741.

Han, D., Leung, Y., and Zhu, J. 2021. Tensile strength and deformational behavior of stylolites and mineral healed joints subject to dynamic direct tension. *Rock Mechanics and Rock Engineering*, 55: 1997-2009. DOI 10.1007/s00603-021-02730-6

Hilgers, C., Koehn, D., Bons, P.D., and Urai J.L. 2001. Development of crystal morphology during unitaxial growth in a progressively widening vein: II. Numerical simulations of the evolution of antitaxial fibrous veins. *Journal of Structural Geology,* 23: 873-885. DOI 10.1016/S0191-8141(00)00160-7

Kaiser, P.K., Amann, F., and Bewick, R.P. 2015. Overcoming challenges of rock mass characterization for underground construction in deep mines. *International Symposium on Rock Mechanics 2015*, ISRM, Montreal, QC, Canada, pp. 15.

Lan, H., Martin, C.D., and Hu, B. 2010. Effect of heterogeneity of brittle rock on micromechanical extensile behavior during compression loading. *Journal of Geophysical Research*, 115: pp. 14. DOI 10.1029/2009JB006496

Li, Y., and Bahrani, N. 2021. A continuum grain-based model for intact and granulated Wombeyan marble. *Computers and Geotechnics*, 129: pp. 21. DOI 10.1016/j.compgeo.2020.103872

Markus, S.L., and Diederichs, M.S. 2022. FEM Models in Stepwise Verification of the FDEM for Simulating Damage around Tunnels in Brittle Rock. *Rocscience International Conference 2021*, Taylor & Francis, Online, 134-140.

Passchier, C. and Trouw, R. 2005. *Microtectonics*, 2nd edn., Springer.

Perras, M.A. and Diederichs M.S. 2014. A review of the tensile strength of rock: Concepts and testing. *Geotechnical and Geological Engineering,* 32: 525-546. DOI 10.1007/s10706-014-9732-0

Potyondy, D.O. and Cundall, P.A. 2004. A bonded-particle model for rock. *International Journal of Rock Mechanics and Mining Sciences*, 41: 1329–1364. DOI 10.1016/j.ijrmms.2004.09.011

Robbiano, F., Liu, K., Zhang, Q.B., and Orellana, L.F. 2022. Dynamic uniaxial compression testing of veined rocks under high strain rates. *International Journal of Rock Mechanics and Mining Sciences,* 153: pp. 13. DOI 10.1016/j.ijrmms.2022.105085

Rocscience 2021. RS2, Version 11.010. Toronto, ON, Canada.

Rógenes, E., Muniz de Farias, M., and Rasmussen, L.L. 2021. The Continuum Voronoi Block Model for simulation of fracture process in hard rocks. *International Journal for Numerical and Analytical Methods in Geomechanics*, 46: 89-112. DOI 10.1002/nag.3292

Sinha, S. and Walton, G. 2020. A study on Bonded Block Model (BBM) complexity for simulation of laboratory-scale stress-strain behavior in granitic rocks. *Computers and Geotechnics,* 118: pp. 20. DOI 10.1016/j.compgeo.2019.103363

Spruzeniece, L., Spath, M., Urai, J.L, Ukar, E., Slezer, M., Nestler, B., and Schewdt, A. 2021. Formation of wide-blocky calcite veins by extreme growth competition. *Journal of the Geological Society,* 178: pp. 17. DOI 10.1144/jgs2020-104

Turichshev, A., and Hadjigeorgiou, J. 2015. Experimental and Numerical Investigations into the Strength of Intact Veined Rock. *Rock Mechanics and Rock Engineering*, 48(5): 1897-1912. DOI 10.1007/s00603-014-0690-x

Turichshev, A., and Hadjigeorgiou, J. 2017. Development of synthetic rock mass bonded block models to simulate the behaviour of intact veined rock. *Geotechnical and Geological Engineering*, 35(1): 313-335. DOI 10.1007/s10706-016-0108-5

Walton, G. 2019. Initial guidelines for the selection of for cohesion-weakening-friction-strengthening (CWFS) analysis of excavations in brittle rock. *Tunnelling and Underground Space Technology,* 84: 189-200. DOI 10.1016/j.tust.2018.11.019